Comparison of Real Time Inference of sEMG with Different Feature Sets via PID and Model Predictive Controller

Jordy Larrea Rodriguez, Caleb Thomson, Jacob George

***Abstract*— Action potentials (AP) are the basis for how neurons communicate in our bodies, our natural circuit. Identifying what those signals mean drives many brain-computer interface (BCI) studies: virtual reality (VR), augmented reality (AR), and projects in the clinical setting (e.g. bionic limbs and human exoskeletons). This study aims to classify the grasping intention detected from one channel of surface electromyography (sEMG) detected at the flexor carpi ulnaris (FCU) with partial integral derivative (PID) control and a simple model predictive controller (MPC). Two models trained with different feature sets, provided inference for reference determination of the controllers. The control signal output from the controller(s) drove a virtual hand in a simulated environment with the control signal either causing all fingers to flex all the way inwards ($control = 1$) or remain relaxed ($control = 0$) with intermediate states. We compared the performance of an MPC with a simple linear plant and a PID controller by calculating the overall distance from a reference square wave. Furthermore, we trialed the performance between MPC control with reference from a Neural Network (NN) trained on one feature and MPC control with reference from a Neural Network trained on five different features. Electrodes were attached to the (FCU) muscle. Participants were tasked with grasping by gripping with digits two through five and relaxing by releasing tension at the stated digits. The performance between PID and our simple MPC produced statistically significant control signals from sEMG inference via five features (p = 2.03e-10); in addition, the inference from models trained with one feature vs five features produced statistically significant results on the performance trials (p = 3.55e-34). There is an inherent need for prosthetic devices that closely resemble actual human biomechanics and human activation via conventional natural processes. Non-linear models such as NN and complex constraint bound hold the potential to classify or infer limb states based on complex and enigmatic neural impulses. Future bionic limbs will likely employ NN architecture for kinematic inference of simulated bio-mechanical systems from either intraneural or EMG signals. VR systems of the future can benefit from sleeves that detect sEMG for real time control in simulations without the equipment of the present day (cameras and controllers).**

Keywords*— Human-Computer Interaction, Real Time Control, Neuroscience

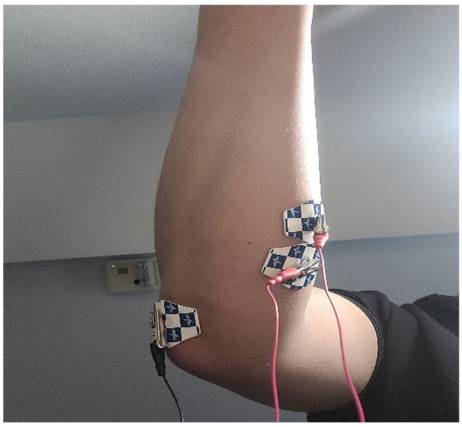

Fig. 1. Electrode configuration for collecting one channel of sEMG from the FCU muscle.

I. Introduction

Individuals suffering from amputation have a significantly reduced quality of life. Furthermore, the alterations to their day to day life often causes victims of amputation to become depressed. Amputees often reject modern prosthetics because they lack life-like qualities and controls often feel unnatural, complicated, or awkward [1-3].

Modern prosthetic devices offer fixed sequences of operation and hardly resemble the complexity and flexibility of physical limb movements [1]. These devices regularly work on detected action of the residual muscle and recorded EMG; however, they depend on assumptions made by simple algorithms. Predictive algorithms, specifically non-linear predictive algorithms can better predict and learn from complex signals such as EMG [1, 3].

Controller algorithms could further integrate the constraints of the biomechanical systems to reproduce actual biomechanical kinematics. MPC for example, integrates the Jacobian of a system and state inputs to predict trajectory in robotics and manufacturing plants. Thus, there is an inherent need to incorporate the actual physics of limb movement with inference from non-linear classifiers of neural signals to reproduce realistic and robust control for prosthetics.

II. Methods

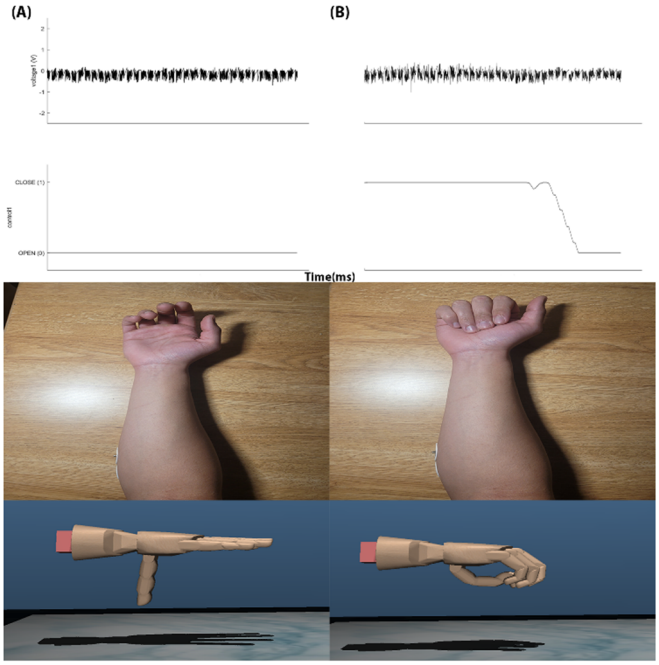

Fig. 2. Control outputs (in milliseconds) via PID with model trained on five feature sets, physical hand positions, and virtual hand positions during hand grasping and hand relaxation. (A) Real-time control output given hand relaxing motion and associated virtual hand position. (B) Real-time control output given hand grasping motion and associated virtual hand position.

Fig. 3. Real time feature set generation for NN inference during hand relaxation and hand grasping motions during a 1.35 second window. Features are normalized so the points are unit-less in the dependent axis. (A) Feature set consisting of one feature at the top and a feature set consisting of five features at the bottom for a window taken during hand relaxation. (B) Feature set consisting of one feature at the top and a feature set consisting of five features at the bottom for a window taken during hand grasping.

Participants

Four participants, ages 21 + 6 years old, were procured for this study. Seventy-five percent of the participants were male with the remaining 25% being female. All participants were of good practical health and did not have any neurological condition. The training sets derived for the NN models were obtained from trails taken of sole participant following poor prediction accuracy.

Neural Network Design

A shallow NN architecture was implemented for this study. The NN consisted of an image input layer, three fully connected layers, two hyperbolic tangent layers, and a regression output layer. The models were trained at a rate of 0.001 for 6 epochs. Binary classification was employed for inference of whether the participant was grasping or not.

Model Training Sets and Feature-Set Generation

Two models were implemented with architecture described above. Data from six trials from the same participants were appended to form a long vector of six training examples. The raw sEMG data was ran through three 2nd order notch filters in series at 60,120, and 180 Hz with Q-factor at 200 Hz. Feature-set one consisted of one generated feature from the filtered sEMG: a moving window absolute average with a window size of 300 samples. Feature-set two incorporated five distinct features: a moving window absolute average, a moving window absolute deviation value, a moving window median, a moving window max, and the root mean squared value of features one through four. The window size was kept at 300 samples for all moving window values (300 ms window size).

The feature sets were generated every 0.2 to 0.6 seconds in real-time and consisted of windows of 1350 samples. Generation of feature-set one took a negligible amount of time to execute, while feature-set two added 0.04 seconds on average to the execution of the loop iteration.

PID Controller Design

The PID controller followed conventional PID structure where the control value, $controlVal$, was determined as:

$$controlVal = k_p * E + IE + k_i * E * dt + k_d * \frac{E - pE}{dt} \quad (1)$$

Where IE, E, and pE are integral error, error, and previous error. Experiments were conducted to determine the optimal gains. Refer to the appendix for specifics of the PID algorithm employed. The goal state was determined by the neural network.

MPC Design, State and Output Functions

A simple architecture for this study's MPC controller was implemented, since the exact constraints and states of the system (hand grasping) were not well understood. The state function reflected the inference of the model during operation and the output function was a simple linear equation that increment or decremented the control value depending on the predicted binary goal reference from the NN. For specifics refer to resources in the appendix of this paper.

Real Time Procedure for Performance Evaluation

Our participant was tasked with relaxing and grasping their hand to match the position of the reproduced control value with a real time square wave overlayed on top of the controller output window. Hand movements were conducted on the limb with electrodes placed at positions shown in Fig. 1. Each trial took approximately three minutes to complete.

Performance Metric Definitions

Performance was evaluated as the difference between the intended signal as determined by the real time square wave and the calculated control value at every point in time during a trial. A total of two trials were conducted for each combination of controller and NN model: MPC and NN trained on feature-set one (config. 1), MPC and NN trained on feature-set two (config. 2), and PID and NN trained on feature-set two (config. 3).

Statistical Analysis of Performance Metrics

Boxplots were generated for comparisons between config. 1 and config. 2 to determine model classification based on feature-set. Furthermore, a boxplot was generated for config. 2 and config. 3 to evaluate relative controller performance on the square wave reference. Datasets were compared via MATLAB's sign-rank test.

III. Results

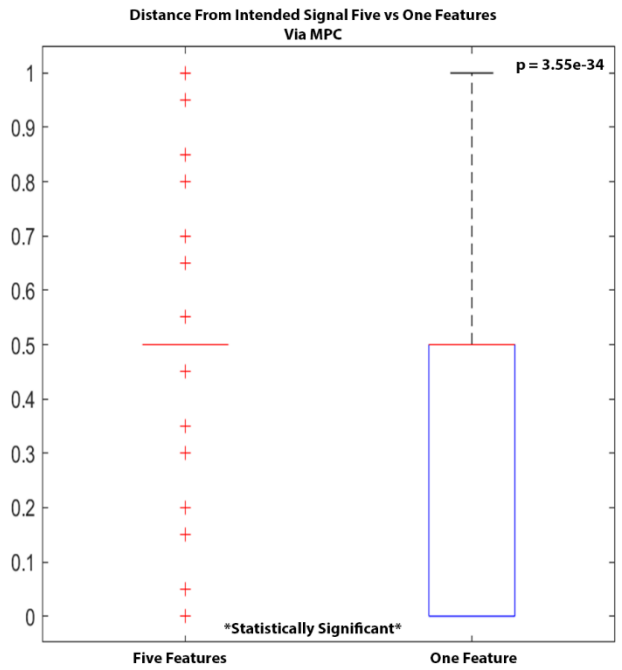

Fig. 4. Boxplot of performance metrics on output of MPC in closed loop with NN trained on feature-set two (left) and NN trained on feature-set one (right).

Model Accuracies

The NN trained on feature-set one that consists of a moving absolute mean window held a prediction accuracy of 90.9% on the training set; however, the performance in real time was quite bad as noted in Fig. 4, where the distance from the intended signal varied a lot. Furthermore, the NN trained on feature-set two consisted of five different features and produced a prediction accuracy of 96.6% on the training set. Performance for the aforementioned model was definitely better than the model trained on the simpler feature-set as noted in the grouping of the points in the plot on the left of Fig. 4.

Results of Performance metric

The performance of the models depending on the complexity of the feature-sets, one V.S. five features, produced statistically significant datasets ($p = 3.55e\text{-}34$, Fig. 4). Fig. 5 denotes statistical significance ($p = 2.03e\text{-}10$) between the performance of the PID and MPC controllers indicating the uniqueness between the control schemes. The real time square-wave favored the mechanics of our simple MPC, so the variance in the PID and the optimal performance of the MPC was expected.

Subjective Impression

Real time inference performance with the feature-set of five features was quite insightful of the high potential NN could serve in classifying sEMG data in real time.

IV. Discussion.

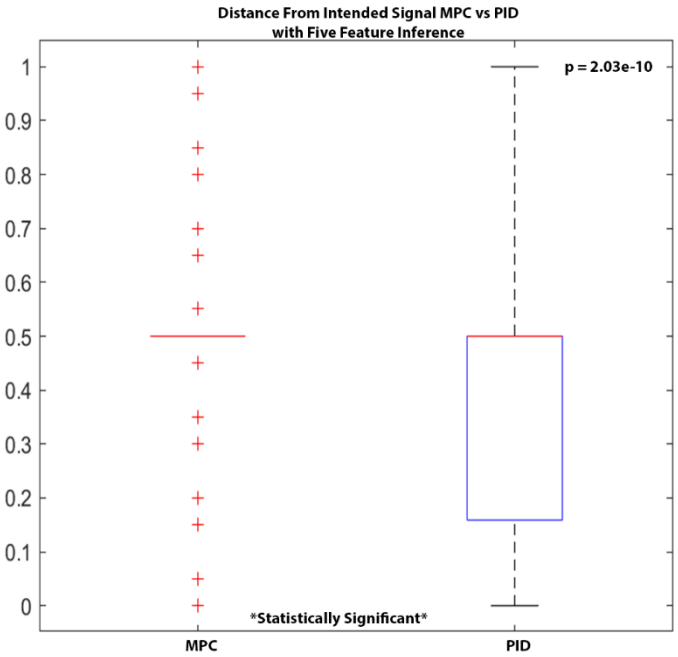

Fig. 5. Boxplot of performance metrics between MPC and PID in closed loop with NN trained on feature-set two.

Summary of Results

The purpose of this work was to showcase the efficacy of NN in classifying sEMG in a closed loop with controller architectures. Performance metrics determined uniqueness between the combinations of systems employed.

Innovation

Our work simulated hand grasping with a closed loop architecture consisting of PID or MPC inputted with inference from a NN all operating in real time. [1] innovated by classifying limb movement with varying degrees of freedom; however, the work did not test their models on sEMG collected in real time. Rather datasets were obtained from online databases.

Future Work and Limitations

Future work should incorporate a PINN component to solve the equations of motion that constrain the bio-mechanics of limbs. An MPC and PINN architecture could then replicate actual limb biomechanics given input from state inference resulting from EMG data.

Broader Implications

Bionic limbs hold the potential to return full functionality to individuals suffering from motor unit damage and limb amputation. Continued research into limb biomechanics and NN applications within the context of neural decoding will ensure a future where prosthetic devices could resemble flesh. Classification of sEMG holds use in AR/VR and the medical industry. Thus, there is an inherent value for continued research in sEMG classification with NN architectures.

APPENDIX I

- Code Repository: KinematicIntentionDecoding

REFERENCES

[1-10]

[1] M. Atzori, M. Cognolato, and H. Muller, "Deep Learning with Convolutional Neural Networks Applied to Electromyography Data: A Resource for the Classification of Movements for Prosthetic Hands," *Front Neurorobot,* vol. 10, p. 9, 2016, doi: 10.3389/fnbot.2016.00009.

[2] I. Batzianoulis, N. E. Krausz, A. M. Simon, L. Hargrove, and A. Billard, "Decoding the grasping intention from electromyography during reaching motions," *J Neuroeng Rehabil,* vol. 15, no. 1, p. 57, Jun 26 2018, doi: 10.1186/s12984-018-0396-5.

[3] D. J. Warren *et al.*, "Recording and decoding for neural prostheses," *Proceedings of the IEEE,* vol. 104, no. 2, pp. 374-391, 2016, doi: 10.1109/jproc.2015.2507180.

[4] N. e. al., "Physics-informed Neural Networks-based Model Predictive Control for Multi-link Manipulators," 2021.

[5] A. Carron, E. Arcari, M. Wermelinger, L. Hewing, M. Hutter, and M. N. Zeilinger, "Data-driven model predictive control for trajectory tracking with a robotic arm," *IEEE Robotics and Automation Letters,* vol. 4, no. 4, pp. 3758-3765, 2019.

[6] F. Djeumou, C. Neary, E. Goubault, S. Putot, and U. Topcu, "Neural Networks with Physics-Informed Architectures and Constraints for Dynamical Systems Modeling," presented at the Proceedings of The 4th Annual Learning for Dynamics and Control Conference, Proceedings of Machine Learning Research, 2022. [Online]. Available: https://proceedings.mlr.press/v168/djeumou22a.html.

[7] L. R. Hochberg *et al.*, "Neuronal ensemble control of prosthetic devices by a human with tetraplegia," *Nature,* vol. 442, no. 7099, pp. 164-71, Jul 13 2006, doi: 10.1038/nature04970.

[8] D. T. Kluger *et al.*, "Virtual Reality Provides an Effective Platform for Functional Evaluations of Closed-Loop Neuromyoelectric Control," *IEEE Trans Neural Syst Rehabil Eng,* vol. 27, no. 5, pp. 876-886, May 2019, doi: 10.1109/TNSRE.2019.2908817.

[9] Y. Smirnov, D. Smirnov, A. Popov, and S. Yakovenko, "Solving musculoskeletal biomechanics with machine learning," *PeerJ Comput Sci,* vol. 7, p. e663, 2021, doi: 10.7717/peerj-cs.663.

[10] D. Yael and I. Bar-Gad, "Filter based phase distortions in extracellular spikes," *PLoS One,* vol. 12, no. 3, p. e0174790, 2017, doi: 10.1371/journal.pone.0174790.